Skilled Human Welder Intelligence Modeling and Control: Part II — Analysis and Control Applications

A search was made to establish a foundation for transferring a skilled human welder's intelligence into a robotic welding system

BY Y. K. LIU, Y. M. ZHANG, AND L. KVIDAHL

ABSTRACT

Transferring a skilled human welder's experiences and skills is an essential step in developing the next-generation intelligent welding machines. In the first part of this study, a skilled human welder's responses to a 3D weld pool surface was modeled. In this second part of the paper, the proposed skilled human welder model is first compared with the novice welder model. The model is then implemented as an intelligent controller to feedback control the gas tungsten arc welding process to maintain a consistent, complete joint penetration. After the initial open-loop control period, the welding current is adjusted by the skilled welder model based on the real-time measured weld pool surface characteristic parameters as well as the welder's previous response. The resultant current waveform, front-side weld pool characteristic parameters, and back-side bead width are recorded/measured and analyzed. It is found that the skilled human welder model can adjust the current appropriately to control the welding process to a desired penetration level despite different initial currents. The controller is also robust against various welding process disturbances, including welding current, arc length, and welding speed disturbance. Compared to the novice welder, the skilled human welder model has a faster convergence time. In addition, no noticeable overshoot is observed. A foundation is thus established for exploring the mechanism and transferring of a skilled human welder's intelligence into a robotic welding system.

Introduction

The goal of this study is to model the skilled welder's response to a 3D weld pool surface, compare the model with that of the novice welder, and utilize the model directly as an intelligent controller to control the welding process as skilled welders do. In the first part of this paper (Ref. 1), the modeling of the skilled human welder is constructed. However, the obtained skilled human welder response model should be further compared with the novice welder model and closed-loop control experiments need to be conducted to verify the effectiveness of the model.

In the gas tungsten arc welding (GTAW) process used in this study, an arc is established between the nonconsumable tungsten electrode and the base metal. The base metal is melted by the arc forming a liquid weld pool that joins the two pieces of base metal together after solidification. The process is relatively slow in comparison with other arc welding processes such as gas metal arc welding (GMAW) such that welders may gradually develop their skills to observe the process and adjust the welding parameters at adequate speeds. Especially for root-pass welding using GTAW as addressed in this study, after the desired complete joint penetration is established, the bottom surface of the workpiece becomes free. The weld pool surface would thus reduce its convexity because part of the melted metal in the weld pool is pushed beyond the bottom surface of the workpiece. The GTAW process is thus suitable for precision joining where accurate real-time controls are needed such as root-pass welding where complete joint penetration typically must be ensured.

Although welders can observe the weld pool surface and adjust the welding parameters accordingly, the model derived from the novice welder's adjustments suffers from large overshoot and oscillation. When adding a low-pass filter, noticeable overshoot is still observed (Ref. 2). On the other hand, adjustments made by skilled welders should not have overshoot nor oscillation as do novice welders. As is shown, the skilled welder model obtained in this study is better than that of the novice welder with faster convergence time and no noticeable overshoot. The model comparison will not only help us to better understand why less skilled welders are not performing as well as skilled welders and help train welders faster in order to resolve the skilled welder shortage issue the manufacturing industry is currently facing (Ref. 3), but will also help us to better control the welding process.

In the second section of this paper, titled Data Analysis and Frequency Response, the data containing both the novice and skilled human welder responses are first analyzed in both time and frequency domains. Linear models are then compared in the third section. In the fourth section, nonlinear neuro-fuzzy models for both novice and skilled welders are compared and the results are analyzed in detail. The skilled human welder model is further utilized as an intelligent controller and a closed-loop control system is developed to provide feedback control of the GTAW process to maintain consistent complete joint penetration in the fifth section, which is titled Control Experiments

Y. K. LIU and Y. M. ZHANG (yuming.zhang@uky.edu) *are with the Institute for Sustainable Manufacturing and Department of Electrical and Computer Engineering, University of Kentucky, Lexington, Ky. L. KVIDAHL is with Huntington Ingalls Industries, Pascagoula, Miss.*

KEYWORDS

Skilled Welder Intelligence
Weld Pool
ANFIS Modeling
Machine Vision
Gas Tungsten Arc Welding (GTAW)

and Analysis. The controller is tested against different initial welding currents and various welding process disturbances, including welding current, arc length, and welding speed disturbance. Finally, the conclusions are drawn.

Data Analysis and Frequency Response

In this section, the data used for constructing both the novice and skilled human welder models are presented/analyzed, and the frequency responses of the skilled welder model (Ref. 1) and novice welder model (Ref. 2) are compared.

Figure 1 depicts the weld pool characteristic parameters and welder's adjustments made by both the novice (Fig. 1A) and skilled welder (Fig. 1B). It has been shown (Refs. 1, 2) that both novice and skilled welders can respond to the fluctuating weld pool surface and control the welding process to a certain degree. It is noticed that the current adjustments made by the novice welder have been filtered before modeling because of the frequently observed abrupt adjustments in the welding current. This is understandable because of the limited skill novice welders possess. For the skilled welder, on the other hand, the current adjustments are considered as correct responses to the changing welding process and are modeled directly. Instead, front-side weld pool characteristic parameters in multiple sampling times are combined and the filtered width, length, and convexity are then used as the model inputs (Ref. 1).

Comparing the adjustments made by novice and skilled welders, it is observed that the novice welder adjustments are generally larger than those of the skilled welder. The maximum current adjustment of the novice welder is about 5 A, while the maximum adjustment of the skilled welder is about 3 A. To better illustrate the different behaviors of novice and skilled welders, frequency analysis was performed and the result is shown in Fig. 2.

It is observed from Fig. 2 that the amplitude of the novice welder frequency response (before filtering) is generally larger than that of the skilled welder. This coincides with the observation from the data plotted in Fig. 1. The novice welder has a larger and more energetic response in all frequencies, indicating the novice welder's frequent underestimation and overestimation of the process. The maximum frequency response of the novice human welder is obtained at 0.1 Hz. However, for the skilled welder, the maximum response is achieved at 0.05 Hz. This implies that the skilled human welder concentrates on the lower frequency more than a novice welder does. After the filter is applied, the low-frequency response of the novice welder is well preserved yet the high-frequency response is largely attenuated. Comparing the filtered novice welder response and skilled human welder response, it is seen that the high-frequency response of the novice welder is significantly lower. This is because the adjustment made by the skilled welder is considered to be relatively accurate and correct, and its moderate response in different frequency ranges including relatively high frequencies is considered to be relevant to the change in the weld pool geometry in different frequencies. As will be seen in the closed-loop control experiments, the skilled human welder model based controller has faster convergence time.

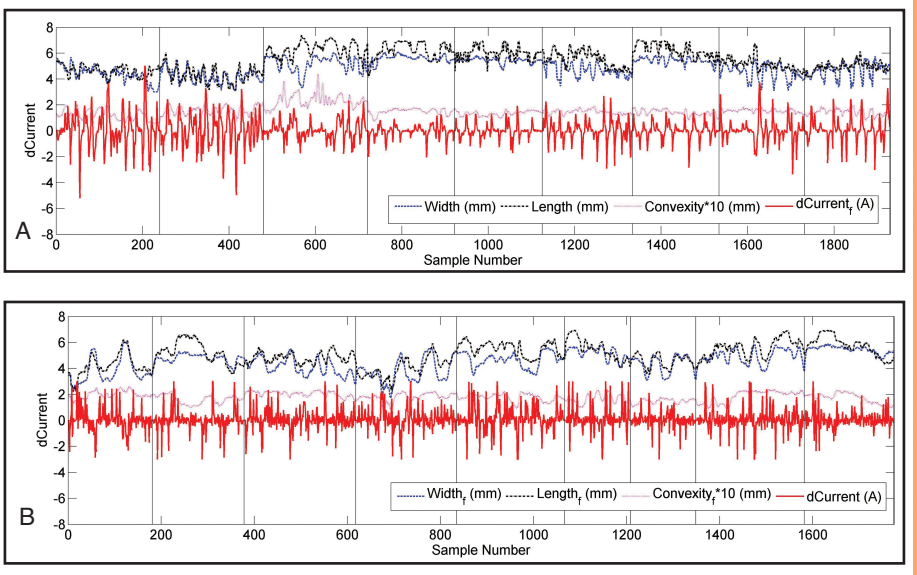

Fig. 1 — Input/output data for constructing welder response models: A — Novice welder model; B — skilled welder model.

Linear Model Comparison

A linear model can sometimes be used as a reasonable approximation of the intrinsic nonlinear model of the welder's response. In this section, the comparison between the novice and skilled human welder linear models is performed and the results are analyzed. The simplicity of linear models will make the comparison rel-

Table 1 — Z-Transfer Functions of the Linear Model

Model	z-transfer function
Novice Human Model (Before Filtering) $H_n(z)=\frac{B_n^W(z)}{A_n(z)}+\frac{B_n^L(z)}{A_n(z)}+\frac{B_n^C(z)}{A_n(z)}$	$A_n(z)=z^3-0.72z^2$ $B_n^W(z)=-0.0492$ $B_n^L(z)=-0.0049$ $B_n^C(z)=-1.735$
Novice Human Model (After Filtering) $H_{nf}(z)=\frac{B_{nf}^W(z)}{A_{nf}(z)}+\frac{B_{nf}^L(z)}{A_{nf}(z)}+\frac{B_{nf}^C(z)}{A_{nf}(z)}$	$A_{nf}(z)=z^3-1.212z^2+0.3558z$ $B_{nf}^W(z)=-0.0246$ $B_{nf}^L(z)=-0.00245$ $B_{nf}^C(z)=-0.8674$
Skilled Human Model $H_s(z)=\frac{B_s^W(z)}{A_s(z)}+\frac{B_s^L(z)}{A_s(z)}+\frac{B_s^C(z)}{A_s(z)}$	$A_s(z)=z^3-0.8562z^2+0.1537z$ $B_s^W(z)=-0.06268$ $B_s^L(z)=-0.003284$ $B_s^C(z)=-0.7247$

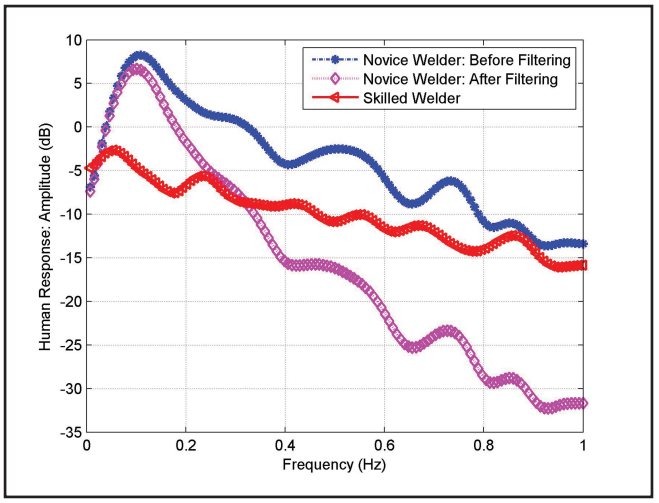

Fig. 2 — Frequency response for the novice and skilled welder.

Table 2 — Poles of the Linear Models

Inputs	Poles
Novice Human Model (Before Filtering)	(0.72, 0, 0)
Novice Human Model (After Filtering)	(0.72, 0.5, 0)
Skilled Human Model	(0.6, 0.26, 0)

atively straightforward and easier to follow.

The identified linear model for the novice and skilled human welder are expressed in Equations 1A and B, respectively:

$$I(k) = -0.049W(k-3) - 0.0049L(k-3) + 1.73C(k-3) + 0.72\,I(k-1) \quad (1A)$$

$$I(k) = -0.16W_f(k-3) - 0.082L_f(k-3) + 1.81C_f(k-3) + 0.26\,I(k-1) \quad (1B)$$

where W, L, and C are the weld pool width, length, and convexity, respectively, and $I(k)$ is the current adjustment by the human welder at instant k. Filtered weld pool width, length, and convexity can be calculated using the following equation (Ref. 1):

$$\mathbf{CP}_f(k) = \alpha_f\mathbf{CP}_f(k-1) + (1-_f)\mathbf{CP}(k) \quad (2)$$

where $\mathbf{CP}_f(k) = [W_f(k), L_f(k), C_f(k)]^T$ and $\mathbf{CP}_f(k-1)$ are the filtered weld pool characteristic parameters at instant k and $k-1$, respectively. $\alpha_f = 0.6$ gives the smallest modeling error and is thus chosen in our study (Ref. 1).

For the novice welder model described in Equation 1A, a low-pass output execution filter is further added to improve the system performance (Ref. 2), which can be expressed as

$$I_f(k) = \alpha_{fo}I_f(k-1) + (1-_{fo})I(k) \quad (3)$$

where $I_f(k)$, $I_f(k-1)$ are the filtered currents at instant k and $k-1$, respectively, and $I(k)$ is the current at instant k. $0<\alpha_{fo}<1$ is the coefficient of the filter, which should be a tradeoff between the filtering effect and response speed. It is found that when $\alpha_{fo}=0.5$, a good tradeoff can be made between the smoothing effect of the filter and the response of the model.

In order to analyze the properties of the linear models, they are written in z-transfer functions (Ref. 4), and are shown in Table 1. The poles and zeros of the z-transfer functions are listed in Table 2.

It is observed that all the poles of the model are inside the unit circle in the Z-plane, which indicates that the model as the controller is asymptotically stable (Ref. 5). In fact, both novice and skilled human welders make adjustments on the welding current as intelligent controllers. Even for a novice welder with limited training who could possibly overestimate or underestime the process, this controller can and should be able to deliver a stable welding process despite his/her limited experience and training. Hence, the models for both novice and skilled welders' responses should be stable. To further analyze the two linear models, impulse responses are calculated and shown in Fig. 3.

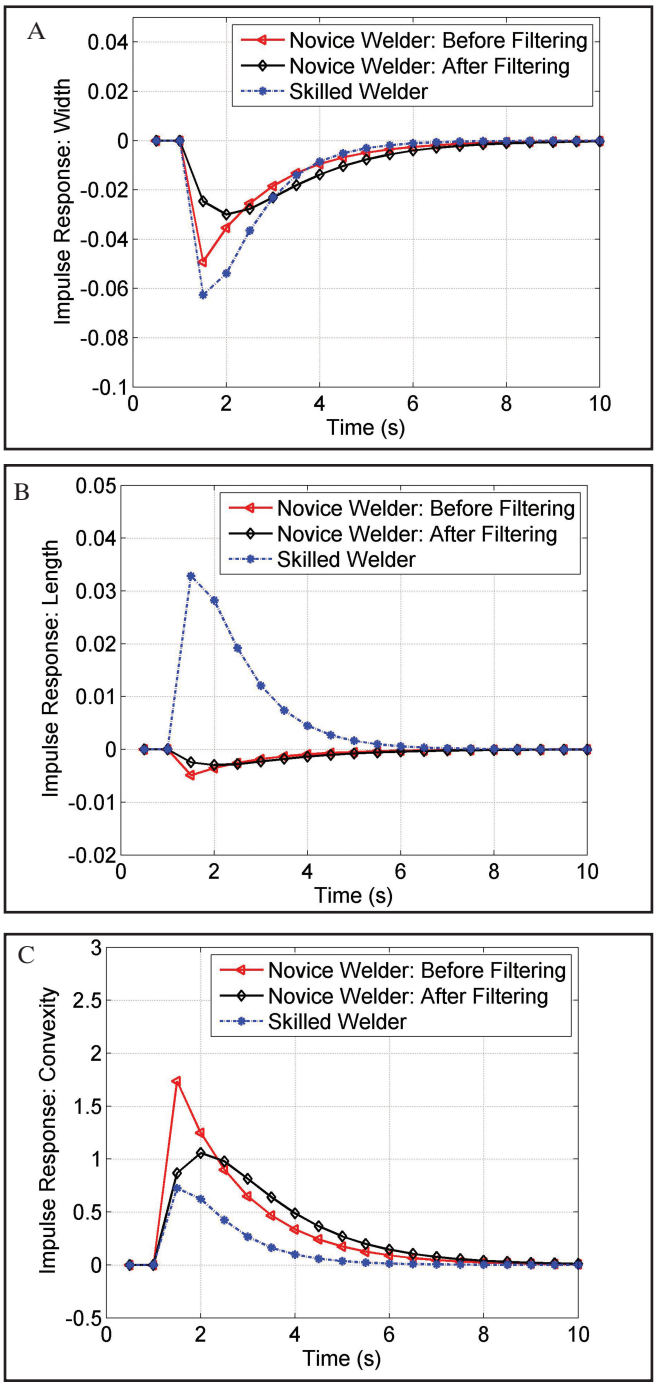

Fig. 3 — Impulse responses of the linear models for novice welder and skilled welder. A — Width impulse response; B — length impulse response; C — convexity impulse response.

Figure 3 depicts the impulse responses of the linear models for both the novice and skilled welder for three inputs (weld pool characteristic parameters). For the width impulse response (Fig. 3A), both the novice and skilled welder react nega-

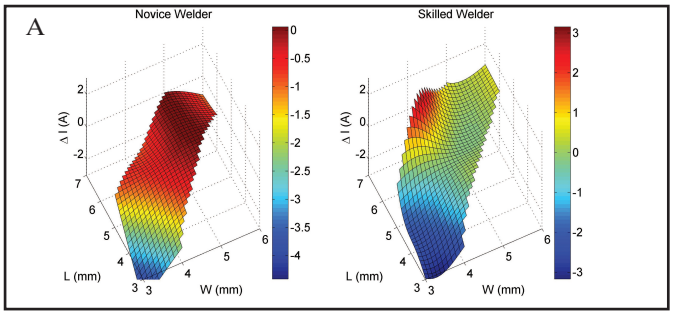

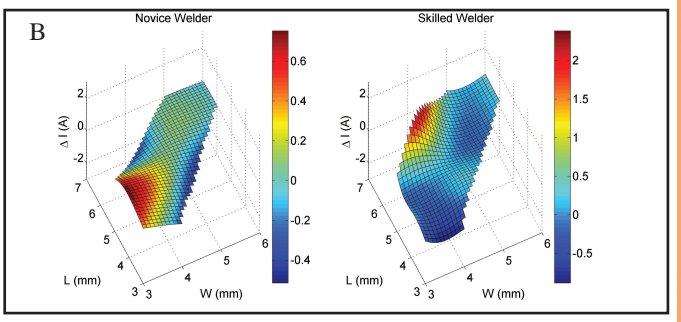

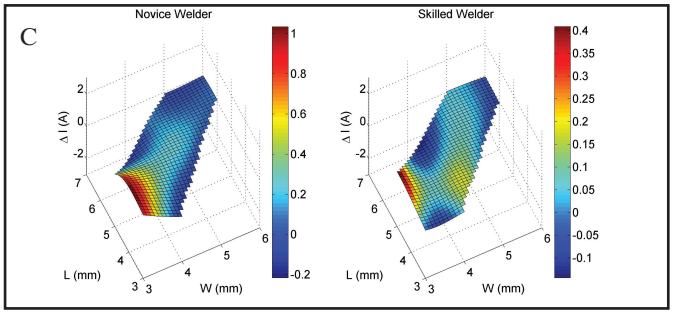

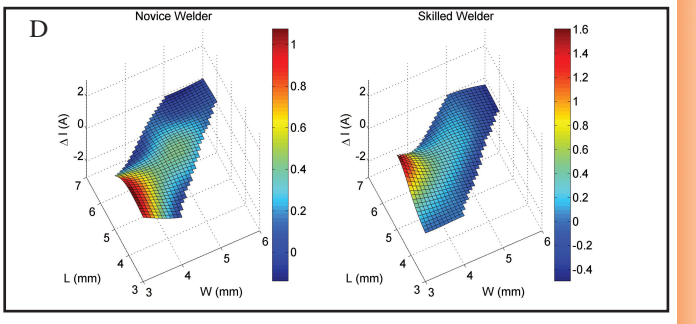

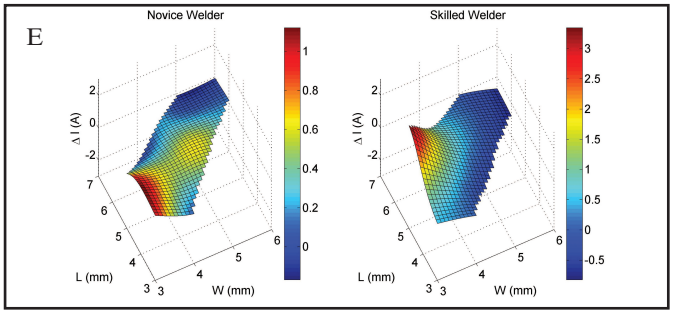

Fig. 4 — Nonlinear model surface of the ANFIS human welder model (left: novice welder; right: skilled welder) for convexity equals A — 0.10 mm; B — 0.14 mm; C — 0.18 mm; D — 0.22 mm; E — 0.26 mm. Previous response is zero for all cases.

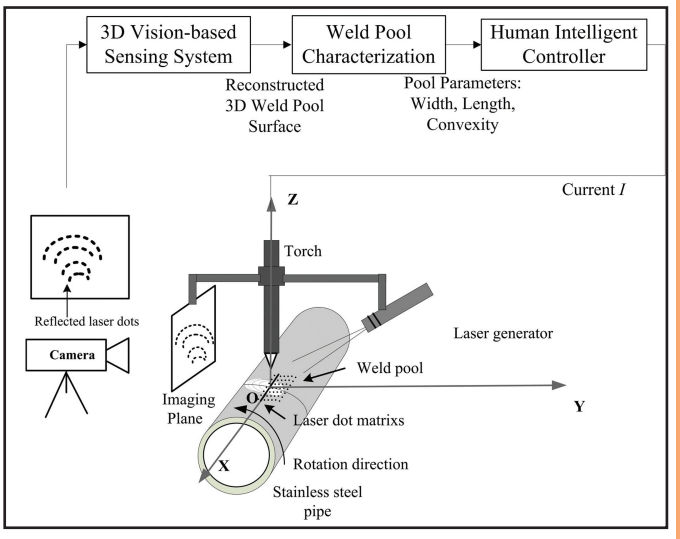

Fig. 5 — Illustration of the closed-loop control system.

tively (decrease the welding current as the weld pool width increases). This is understandable because the increase in width generally indicates an increase in weld penetration, and the average effect of the welder response should be negative to compensate for this positive increment in weld pool width. However, the magnitude of the impulse response (i.e., the static gain of the linear model) is different. The skilled welder model reacts larger to the width increase (with static gain of 0.06 A/mm) than the novice welder (with static gain of 0.049 A/mm). After filtering, the static gain of the novice welder is further reduced to 0.025 A/mm. On the other hand, the skilled welder model has slightly shorter settling time (about 5 s) compared to that of the novice welder model after filtering (about 6 s). For the weld pool length (Fig. 3B), the skilled welder reacts differently than the novice welder. The novice welder is not sensitive to the length increase, and the adjustment is minimal (with maximum magnitude of 0.003 A corresponding to a 1-mm length increase). For the skilled welder, the response to the length is much more significant (with maximum magnitude of 0.033 A corresponding to a 1-mm length increase). The positive impulse response indicates the average effect of the adjustment made by the skilled welder is positive (i.e., increase the current as the weld pool length increases). This makes sense because the increase in length may indicate the increase in welding speed and decrease in total heat input into the process, especially when the weld penetration is sufficient. In this case, the welding current should be increased to compensate for the increase in weld pool length. Figure 3C shows the impulse response for the weld pool convexity input. Both novice and skilled welders react to the convexity with positive adjustments. This is understandable because the increase in convexity generally indicates a decrease in weld penetration. In this sense, the welder should increase the current to compensate for this effect. After the filter, the novice welder model reacts to the convexity less energetically and more smoothly. Comparing the convexity impulse response made by the skilled and novice welders, it is observed that the skilled welder model has a much shorter settling time (about 5 s) than that of the novice welder after filtering (about 7 s).

It is thus clear that the linear model derived from the skilled human welder response has better performance than that derived from the novice human welder in terms of settling time. The difference between the impulse response relative to the weld pool width, length, and convexity also indicates the different adjustments made by novice and skilled welders. In particular, the skilled welder responds to the weld pool length while the novice welder does not noticeably. The skilled welder thus not only responds faster and more accurately, but also makes use of more information

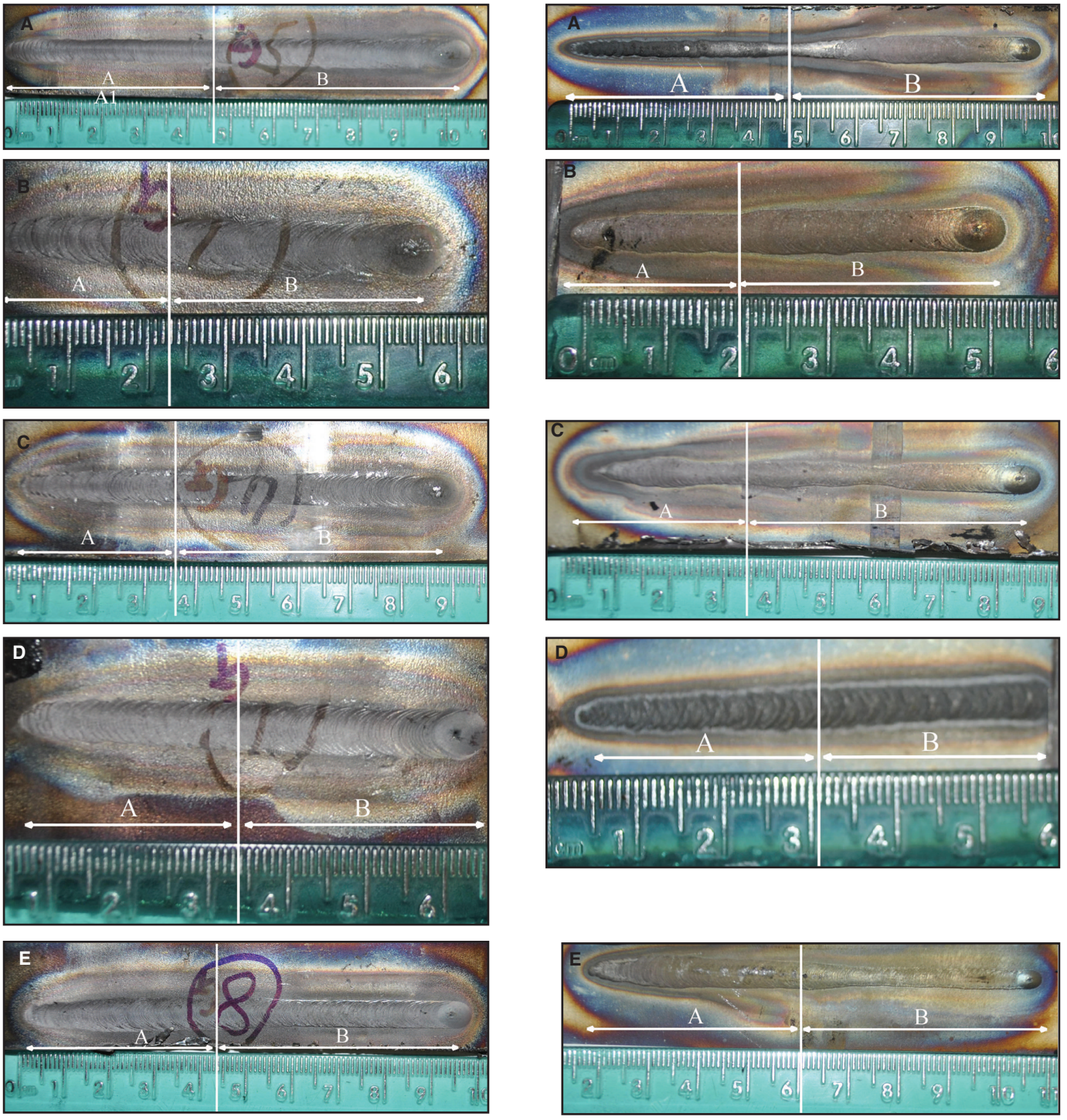

Fig. 6 — Front-side and back-side weld bead from initial current experiments with initial current: A — 52 A; B — 54 A; C — 56 A; D — 58 A; E — 62 A. Left: front-side weld bead; right: back-side bead width. (The experiment in C is made without gas purging intentionally to examine the robustness of the response model against possible manufacturing condition faults.)

from the weld pool.

Nonlinear Model Comparison

Although linear models can give us some knowledge about the difference between novice and skilled welders, it is inevitable that the linear model can only model the average effect of the input parameters over the output. Detailed information is lost because of the incapability of linear modeling. In the following, the proposed nonlinear ANFIS models for both novice and skilled welders are compared, and the results are analyzed in detail.

Figure 4 demonstrates the proposed neural fuzzy model surface for different weld pool geometries. It is observed that nonlinearity is substantial in modeling the human welder's response to 3D weld pool geometry. Careful observation in Fig. 4 shows that when the weld pool convexity is small (i.e., the convexity equals 0.1 mm in Fig. 4A), the current adjustments are negative for both small and large weld pool area, while approaching zero for medium weld pool area (with the weld pool width at about 5 mm, and length at about 5 mm). Actually, such small convexity for small weld pool size generally indicates over-

penetration and the human welder should decrease the current to prevent melt-through. Comparing the response of the novice welder to that of the skilled welder, it is observed that the difference appears when the width is small yet the length is relatively large (i.e., the length-to-width ratio is large). The novice welder is not sensitive to this scenario, and the adjustments are minimal. For the skilled welder, on the other hand, the current adjustment is positive, with the largest adjustments of 3 A. It makes sense because when the length-to-width ratio is large, and the convexity is small, it indicates that the penetration is not sufficient because of the insufficient total heat input. The large length is probably caused by the fast welding speed. In this case, the welder should increase the current to compensate for this underpenetration. Moreover, this phenomenon indicates the nonlinear inference of the human welder's response rather than the linear approximation of the correlation provided by the linear models. As the convexity becomes larger (Fig. 4C), the adjustment made by the skilled welder is generally smaller than that of the novice welder. This indicates that the skilled welder tends to not adjust the current since the convexity is within the tolerance range. Figure 4E depicts the case when the weld pool convexity is relatively large. In this case, the skilled welder's current adjustment is larger than that of the novice welder. This implies that for this extreme case, the skilled welder is more sensitive and the large response represents the correct adjustment made by the human welder. It is observed that for all cases the nonlinearity is substantial and the nonlinear ANFIS model does provide detailed knowledge about the adjustments made by the skilled welder. This highly nonlinear adjustment made by the skilled welder is thus crucial to producing quality welds and mechanizing the human welder's intelligence.

It is observed from Fig. 4 that in normal cases the skilled welder's adjustments are minimal, which can prevent the large oscillation and overshoot from which the novice welder model suffers. However, in other cases where the convexity is either considerably small or large, the adjustment made by the skilled welder is larger than that of the novice welder, which can provide shorter settling time than a novice welder does. The skilled welder model does provide better adjustment than the novice welder. In the next section, closed-loop control experiments are conducted to further verify the effectiveness of the skilled human welder model under various welding process disturbances and variations.

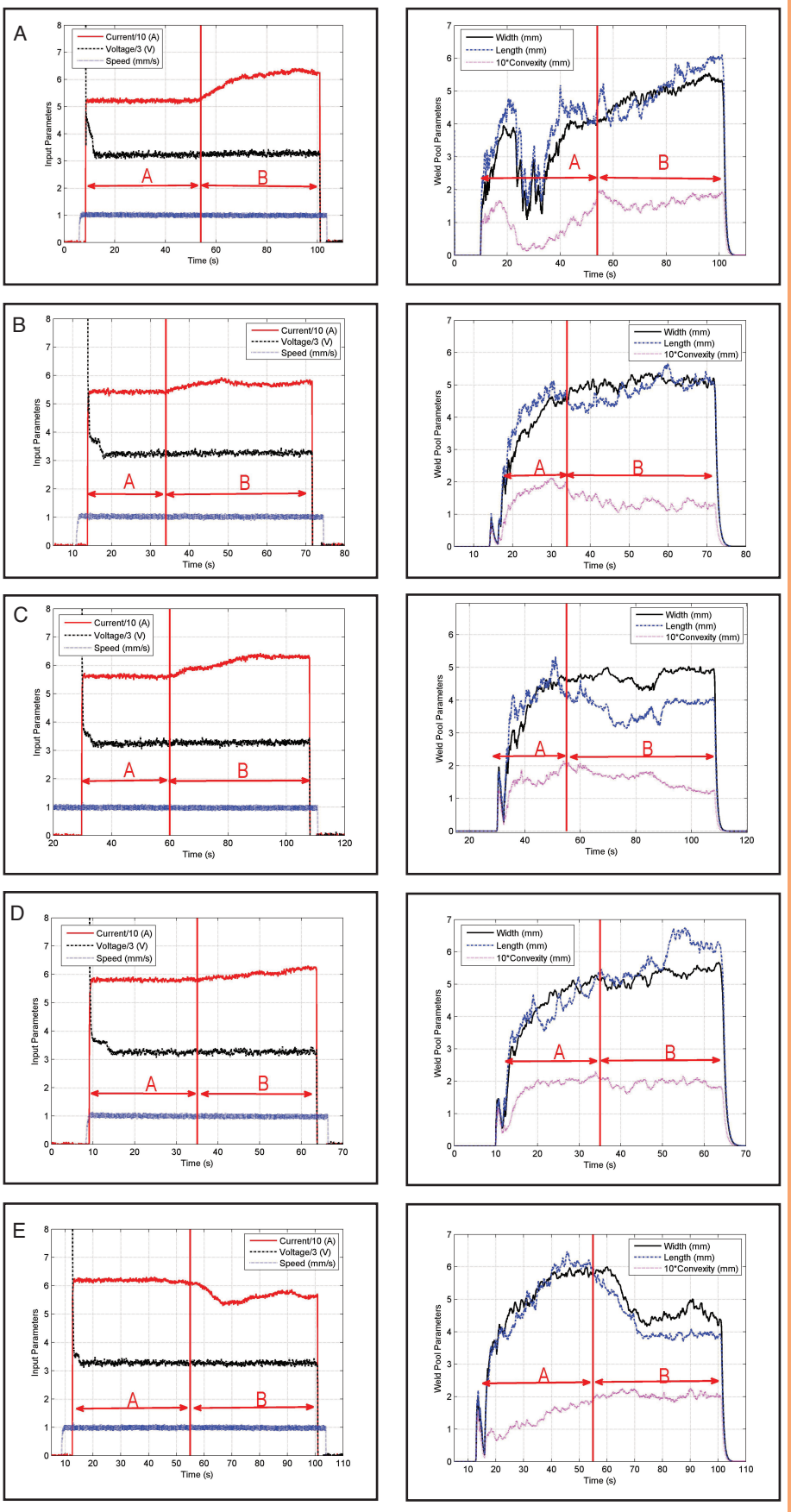

Fig. 7 — Control signals and weld pool characteristic parameters with different initial currents: A — 52 A; B — 54 A; C — 56 A; D — 58 A; E — 62 A. Left: control signals; right: real-time measured front-side weld pool characteristic parameters.

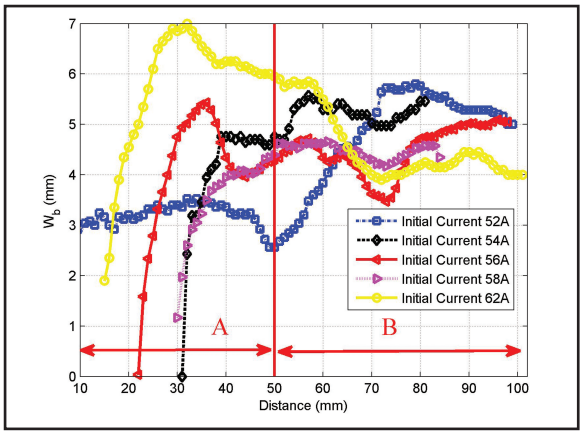

Fig. 8 — Offline measured back-side bead width for different initial current experiments.

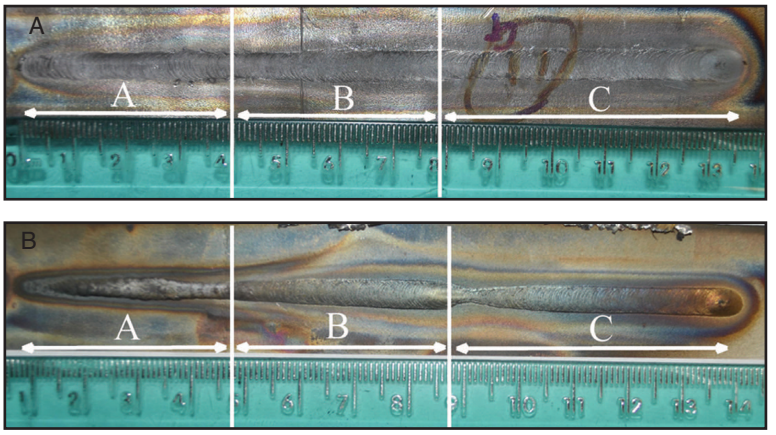

Fig. 9 — Front-side and backside weld bead appearances for current disturbance experiment. A — Front-side weld bead; B — backside weld bead.

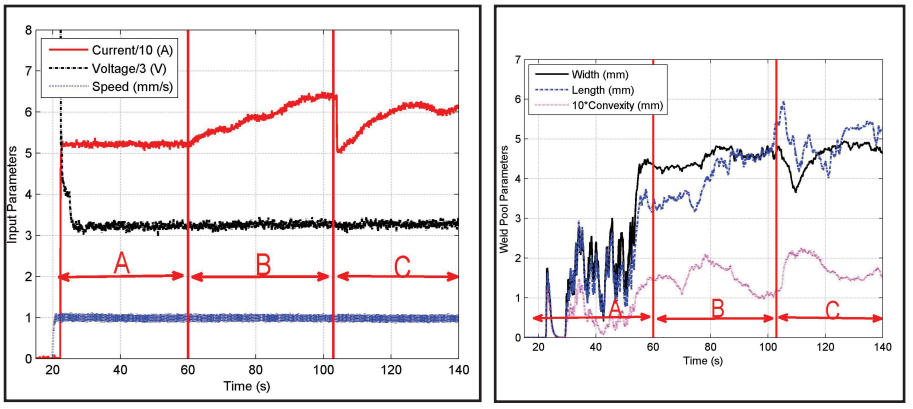

Fig. 10 — Control signals and weld pool characteristic parameters for current disturbance experiment. Left: Control signals; right: real-time measured front-side weld pool characteristic parameters.

Control Experiments and Analysis

The developed closed-loop control system is illustrated in Fig. 5. In this experimental system, the pipe weld application is made using direct current electrode-negative GTAW. The pipe material is 304 stainless steel. The outer diameter and wall thickness of the pipe are 113.5 and 2.03 mm, respectively. The pipe rotates during the experiment while the positions of the torch, imaging plane, laser structure light generator, and camera are fixed in space. A computer controls the rotation speed and torch motion to achieve the required welding speed and arc length.

A computer connected to the camera processes the captured image, reconstructs the weld pool, and extracts three characteristic parameters of the weld pool (width, length, and convexity) in real-time. The skilled human intelligence model then output the current. To imitate the welder's behavior as in the human welder's response principle detailed in the first part of this study, in each experiment an initial welding input is first applied for the weld pool to grow and complete joint penetration is achieved. Then the closed-loop control period of the human intelligence model starts. The experimental parameters (including welding parameters and imaging/monitoring parameters) used in the closed-loop control experiments are the same as those listed in the first part of this study.

To confirm the effectiveness of the proposed skilled human welder model in controlling the GTAW process to achieve the desired weld penetration, various closed-loop control experiments have been designed and conducted in this section. In the first subsection, the experiments with different initial currents are conducted. The robustness of the human welder response model-based control with respect to the initial current is analyzed. In the second subsection, the current disturbance is applied and the controller's robustness against current disturbance is tested. In the third and fourth subsections that follow, the robustness of the proposed controller against arc voltage and welding speed disturbances are further verified.

Robustness with Initial Current

Experiments with different initial welding currents were conducted in this subsection to test the robustness of the controller against different initial conditions. Five experiments were conducted, with initial current set to 52, 54, 56, 58, and 62 A. The arc length was set at 5 mm and the welding speed was 1 mm/s in all five experiments. The front-side and back-side weld beads obtained are shown in Fig. 6. The control inputs and real-time measured front-side weld pool characteristic parameters in these three experiments are plotted in Fig. 7. The offline measured back-side bead widths for five experiments are depicted in Fig. 8. In these figures, the open-loop and closed-loop periods are identified as A and B, respectively. The vertical line indicates the start of the closed-loop control.

As can be observed from Fig. 8, the proposed intelligent human controller can drive the back-side bead width to a desired value (i.e., about 5 mm) despite the differences in initial current. The deviation of the back-side bead width in these five experiments is about 1 mm, which is considered acceptable in our application. Compared to the novice human welder response model-based controller in Ref. 2, the skilled human welder model can achieve a shorter convergence/settling time.

Specifically, for the initial current of 52 A, the back-side bead width at the end of the open-loop period is about 2.5 mm (Fig. 8), which is considered insufficient penetration in our application. The corresponding weld pool width, length, and convexity (Fig. 7A) are 4, 4, and 0.2 mm, respectively. Then the skilled human welder model is utilized to calculate the current adjustments applied to the system. The current reaches its steady-state (about 61 A) in 15 s. The front-side weld pool width, length, and convexity are about 5, 5, and 0.15 mm, respectively. The back-side bead width is controlled at about 5 mm. Similarly, for an initial current of 54, 56, 58, and 62 A, the proposed model is able to control the back-side bead width accordingly to achieve the desired

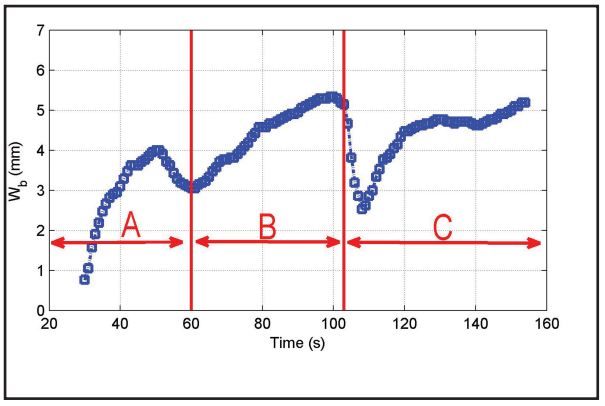

Fig. 11 — Offline measured back-side bead width for current disturbance experiment.

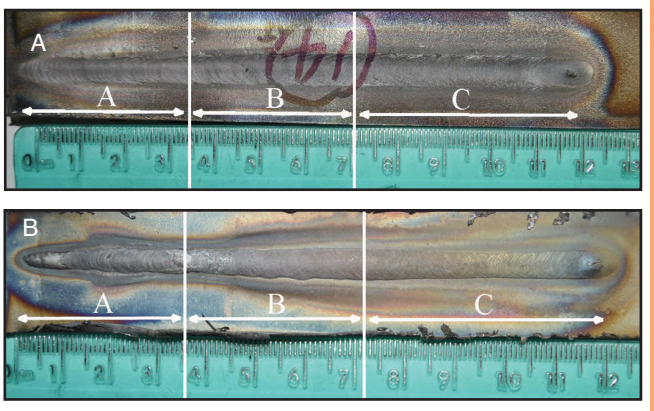

Fig. 12 — Front-side and backside weld bead appearances for arc length disturbance experiment. A — Front-side weld bead; B — backside weld bead.

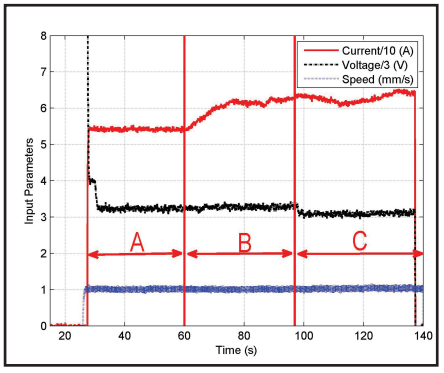

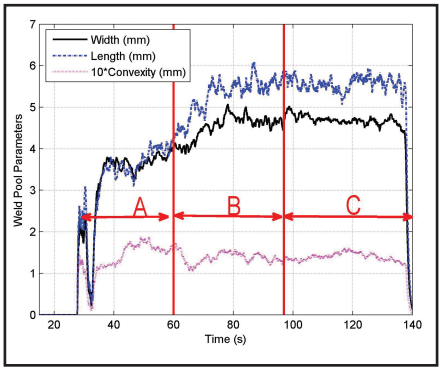

Fig. 13 — Control signals and weld pool characteristic parameters for arc length disturbance experiment. Left: Control signals; right: real-time measured front-side weld pool characteristic parameters.

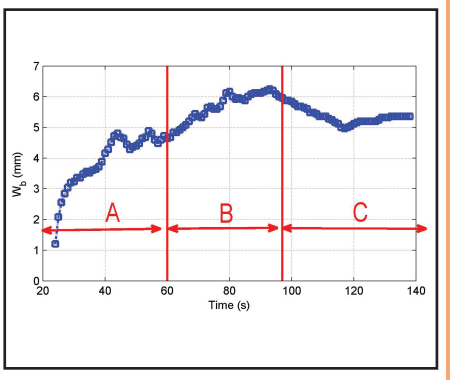

Fig. 14 — Offline measured back-side bead width for arc length disturbance experiment.

penetration. It is noticed that the steady-state current is slightly different in each experiment (61 A for initial current of 52 A, 57 A for initial current of 54 A, 60 A for initial current of 56 A, 60 A for initial current of 58 A, and 55 A for initial current of 62 A). This is understandable because a skilled human welder adjusts the current based on his/her observation of the welding process. The back-side bead width controlled by the proposed model is about 5 mm with 1-mm deviation, which is considered acceptable in our application.

It was noticed in Experiment 3 with an initial current of 56 A that the controller is able to control the process to the desired penetration states with 59 A after the closed-loop control started — Fig. 7. At 70 s, however, unmodeled welding process variation occurred. Accordingly, the back-side bead width decreased from 4.6 to 3.6 mm. The corresponding front-side weld pool width, length, and convexity decreased from 5, 5, and 0.2 mm to 4.5, 3.5, and 1.7 mm, respectively, indicating a smaller weld pool and insufficient penetration. The controller was able to increase the current to a new steady state (about 62 A) in order to control the back-side bead width back to 5 mm. The controller's robustness against unmodeled process variations was demonstrated.

In Experiment 4 with an initial current of 58 A, the inside of the pipe was intentionally not protected with purging gas. It is observed from Fig. 8 that the back-side bead width was controlled at about 4.5 mm, which is considered acceptable in our application. In other experiments, the inside of the pipe was well protected with purging gas. The robustness of the controller in achieving desired penetration with respect to different back-side protection conditions was thus verified.

Current Disturbance

In this subsection, the controller's robustness against current disturbance is investigated. The arc length and welding speed were set at 5 and 1 mm/s, respectively. The experimental results are presented in Figs. 9–11. The process begins with an open-loop period of about 38 s (period A with initial current of 52 A), which brings the back–side bead width to about 3 mm. In the first 42 s after the open-loop period, no error existed between the calculated current and applied current. The skilled human welder model was able to control the back-side bead width to about 5 mm (Fig. 11) by increasing the current to about 62 A — Fig. 10. The corresponding front-side weld pool parameters were 4.8, 4.8, and 0.1 mm. In t = 103 s, the current disturbance was applied. The welding current was set at 50 A, which is about 12 A smaller than the calculated current. As a result, the weld pool width decreased to about 3.8 mm, the length first increased and then decreased to 4.2 mm, and the convexity increased from 0.1 to 0.2 mm. The change in the front-side weld pool characteristic parameters indicated that the weld penetration became smaller. The skilled human welder model was able to adjust the welding current to about 61 A in an effort to compensate for this artificial current disturbance (Fig. 10), and the back-side bead width could be maintained at around 5 mm. The controller's robustness against welding current disturbance was thus verified.

Arc Length Disturbance

Arc length is another welding process input that has impact on the weld pool geometrical appearance and penetration state. In this subsection, the robustness of the proposed intelligent controller with arc length disturbance is examined.

In this experiment, the initial arc length was 5 mm and the initial welding current was 56 A. The open-loop period started from 28 to 60 s (marked by period A in Fig. 13). At the end of the open-loop period,

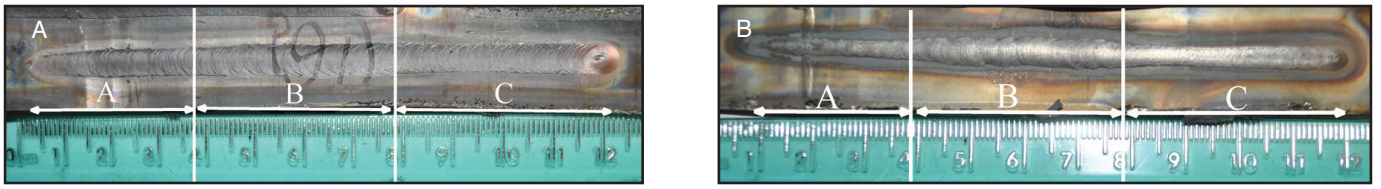

Fig. 15 — Front-side and backside weld bead appearances for speed disturbance experiment. A — Front-side weld bead; B — backside weld bead.

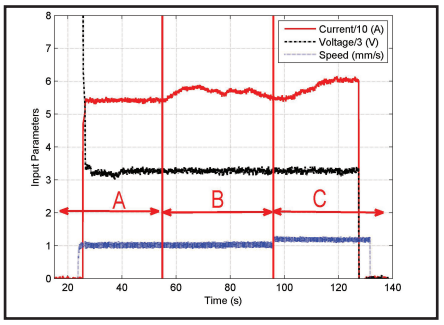

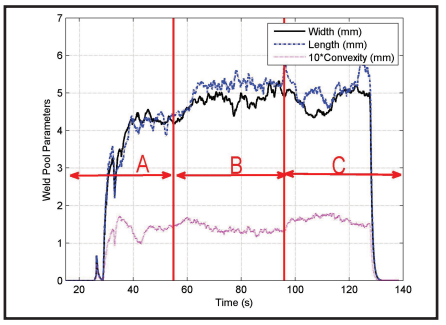

Fig. 16 — Control signals and weld pool characteristic parameters for welding speed disturbance experiment. Left: Control signals; right: real-time measured front-side weld pool characteristic parameters.

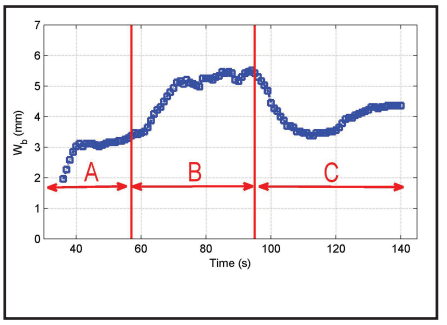

Fig. 17 — Offline measured backside bead width for welding speed disturbance experiment.

the front-side weld pool width, length, and convexity were 4, 4, and 0.15 mm, and the back-side bead width was 4.8 mm. Then the closed-loop control started. The front-side weld pool width, length, and convexity were controlled at 4.8, 5.8, and 0.13 mm, and the back-side bead width was about 6 mm. At t = 96 s, the arc length changed to 3.5 mm. As a result, the weld pool width immediately increased. If the current is unchanged (i.e., 62 A in Fig. 13), the penetration state increases and possible melt-through may occur. As can be observed in Fig. 13, by decreasing the current, the closed-loop control system successfully eliminates the influence of the arc length variation and the resultant back-side bead width is about 5 mm. The front-side weld pool width, length, and convexity were maintained at 4.8, 5.5, and 1.3 mm, respectively.

Welding Speed Disturbance

In arc welding, the welding speed is a major factor that influences heat input into the process and has great impact on weld penetration. In this experiment, a step change of the welding speed was applied to examine the robustness of the controller over variations in travel speed. The experimental results are shown in Figs. 15–17. After an open-loop period (marked by A), the controller was applied and the back-side bead width was increased from 3 mm (at the end of the open-loop period) to 5 mm. During the first 40 s of the closed-loop period (marked by B in these figures), the travel speed was 1 mm/s. Then the speed was changed to 1.1 mm/s in the second part of the closed-loop control (marked by C). As can be observed from Fig. 16, the weld pool width and length immediately decreased, while the weld pool convexity increased due to the step change of the speed. This change in the weld pool characteristic parameters indicates a decrease in the weld penetration specified by the back-side bead width. The controller was able to increase the current according to this abrupt change in the weld pool and tried to maintain a constant complete joint penetration. As can be seen in Fig. 16, the current increased from 58 A (when the travel speed was 1 mm/s) to about 60 A (when the travel speed was 1.1 mm/s). As a result, the back-side bead width was adjusted back to about 4.5 mm.

It was noticed that despite various welding process disturbances, the skilled human welder response model was able to control the welding process within the desired penetration state (5 mm with about 1 mm deviation). The robustness of the proposed intelligent controller was thus verified.

Conclusion

Analysis based on linear models for novice and skilled welders suggests that the skilled welder not only responds faster and more accurately but also makes use of more information from the weld pool. Further analysis based on nonlinear models reveals that in normal cases the skilled welder's adjustments are minimal to prevent the large oscillation and overshoot the novice welder model suffers, while in other cases where the convexity is either considerably smaller or larger, the adjustment made by the skilled welder is larger than that of the novice welder, which can provide for a shorter settling time. The effectiveness and robustness of the proposed model-based intelligent controller has been verified with different initial current and various welding process variations/disturbances, including welding current, voltage, and welding speed disturbances. The skilled welder model obtained in this study performs better than that of the novice welder with faster convergence time, and no noticeable overshoot. A foundation is thus established to explore the mechanism and transformation of the human welder's intelligence into a robotic welding system.

Acknowledgments

This work was funded by the National Science Foundation under grant CMMI-0927707 and IIS-1208420.YuKang Liu would like to thank WeiJie Zhang and Benny Porter for their assistance in conducting experiments.

References

1. Liu, Y. K., and Zhang, Y. M. 2014. Skilled human welder intelligence modeling and control: Part I — Modeling. *Welding Journal* 93(2): 46-s to 52-s.

2. Liu, Y. K., Zhang, W. J., and Zhang, Y. M. 2013. Neuro-fuzzy based human intelligence modeling and robust control in gas tungsten arc welding process. *Proc. 2013 American Control Conference*, Washington, D.C., June 17–19.

3. Uttrachi, G. D. 2007. Welder shortage requires new thinking. *Welding Journal* 86(1): 6.

4. Cornelius, T. L. 1996. Digital control systems implementation and computational techniques. *Academic Press*.

5. Chen, C. T. 1999. *Linear System Theory and Design* (3rd Ed.). Oxford University Press.

6. Ljung, L. 1999. *System Identification — Theory for the User*, 2nd edition. PTR Prentice Hall, Upper Saddle River, N.J.